Synergistic Day-Ahead Scheduling Framework for Smart Distribution Grid Under Uncertainty

Kasi Vemalaiah, *Graduate Student Member, IEEE*, Dheeraj Kumar Khatod, *Member, IEEE*, and Narayana Prasad Padhy, *Senior Member, IEEE*

***Abstract*—Under the smart grid environment, implementation of load management programs, integration of active elements, and associated uncertainties have increased the complexity in operation and management of the existing distribution networks many folds as before. Therefore, for optimal operation of such a complicated distribution network, this article proposes a synergistic day-ahead scheduling scheme emphasizing the combined impact of network reconfiguration, active elements, and demand response. Minimizing the overall cost associated with the operation and management of distribution system, the formulation is proposed as a mixed-integer second-order cone programming problem. This formulation captures the exact characteristics of power flow in network and ensures its fast convergence to global optima. Further, the Benders decomposition method is employed to deal with computational complexities in achieving a solution. Test results on a modified IEEE 33-bus network show notable enhancement in the techno-economic performance of the network.**

***Index Terms*—Energy management, network reconfiguration, smart distribution grid (SDG), stochastic convex programming, synergistic day-ahead scheduling (SDAS), uncertainty.**

NOMENCLATURE

Indices and Sets

T/Ω	Set of time intervals/scenarios.
$\Phi/\Phi^{\mathrm{LD}}/\Phi^{\mathrm{SS}}$	Set of network/load/sub station buses.
$\Phi^{\mathrm{BS}}/\Phi^{\mathrm{SCB}}$	Set of buses coupled with BESS/SCB.
$\Phi^{\mathrm{PV}}/\Phi^{\mathrm{WT}}$	Set of buses coupled with PVG/WTG.
Φ^{i}	Set of buses connected to ith bus.
i,j	Index for the bus.
ij,l	Index for the branch.
t,ω	Index for time, scenario.

Parameters

$\alpha^{\mathrm{g}}_{i,t}/\beta^{\mathrm{g}}_{i,t}$	Shape parameters corresponding beta PDF.
$\eta^{\mathrm{CH}}_{i}/\eta^{\mathrm{DIS}}_{i}$	Charging/discharging efficiency of ith BESS.
$\kappa^{\mathrm{SL,UP}}_{i}/\kappa^{\mathrm{SL,DN}}_{i}$	Fraction of load forecast at ith SL available for load shifting (up/down).
$\mu^{g}_{i,t}/\sigma^{g}_{i,t}$	Mean/Standard deviation value of ith PVG/WTG at tth time interval.
τ_{ω}	Probability of scenario ω.
C^{CSW}_{ij}	Operational and maintenance cost of ijth CSW.
$C^{\mathrm{BS}}_{i}/C^{\mathrm{SCB}}_{i}$	Operational and maintenance cost of ith BESS/SCB.
C^{CL}_{i}	Cost of energy not served in ith CL.
$C^{\mathrm{SL,UP}}_{i}/C^{\mathrm{SL,DN}}_{i}$	Cost of incentive provided for up/down of consumption in ith SL.
$C^{\mathrm{SS}}_{t,\omega}/\kappa^{\mathrm{SS}}_{q}$	Price of active power purchased from the upper grid and its corresponding reactive component.
$E^{\mathrm{BS}}_{i,\min}/E^{\mathrm{BS}}_{i,\max}$	Lower and upper energy capacity bounds for the ith BESS.
$I_{ij,\max}$	The upper current restriction for the ijth line.
$N^{\mathrm{SCB}}_{i,\max}/\Psi^{\mathrm{SCB}}_{i,\max}$	Highest allowable count of daily switching operations/the number of available banks for the ith SCB.
$N^{\mathrm{CSW}}_{ij,\max}$	Highest allowable count of daily switching operations for the ijth CSW.
$P^{\mathrm{SS}}_{i,\min}/P^{\mathrm{SS}}_{i,\max}$	Active power bounds of sub-station (upper grid).
$P^{\mathrm{LD}}_{i,t}/\Theta^{\mathrm{SL}}_{i,t}$	Forecast of demand/ power factor angle of ith SL.
$P^{\mathrm{PV}}_{i,t}/P^{\mathrm{WT}}_{i,t}$	Forecast of ith PVG/WTG.
$P^{\mathrm{CAP}}_{i,t}/P^{\mathrm{g}}_{i,t}$	Capacity/Forecast of ith PVG/WTG.
$P_{ij,\max}/Q_{ij,\max}$	Active/Reactive power bounds of ijth line.
$Q^{\mathrm{SS}}_{i,\min}/Q^{\mathrm{SS}}_{i,\max}$	Reactive power bounds of substation (upper grid).
$Q^{\mathrm{SCB}}_{i,\mathrm{step}}/\rho^{\mathrm{SCB}}_{i,init}$	Step size/initial step of ith SCB.

Manuscript received 29 August 2023; revised 9 January 2024 and 28 February 2024; accepted 12 March 2024. This work was supported in part by the Department of Science and Technology, India, through the research grants: Indo–Danish collaboration for data-driven control and optimization for a highly Efficient Distribution Grid ID-EDGe under Grant DST-1390-EED, in part by the US–India Collaborative for Smart Distribution System With Storage UI-ASSIST under Grant IUS-1132-EED, and in part by the Parameter and Topology Estimation of Distribution Network under Grant SER-1667-EED. Paper no. TII-23-3306. *(Corresponding author: Kasi Vemalaiah.)*

Kasi Vemalaiah and Dheeraj Kumar Khatod are with the Electrical Engineering Department (EED), Indian Institute of Technology (IIT) Roorkee, Roorkee, Uttarakhand 247667, India (e-mail: kasi_v@ee.iitr.ac.in; dheeraj.khatod@ee.iitr.ac.in).

Narayana Prasad Padhy is with the EED, IIT Roorkee, Roorkee, Uttarakhand 247667, India, and also with the Malaviya National Institute of Technology Jaipur, Jaipur, Rajasthan 302017, India (e-mail: nppadhy@ee.iitr.ac.in).

Color versions of one or more figures in this article are available at https://doi.org/10.1109/TII.2024.3385366.

Digital Object Identifier 10.1109/TII.2024.3385366

r_{ij}/x_{ij} Resistance/reactance of ijth line.
$S^{\text{BS}}_{i,\max}$ Apparent power rating of ith BESS.
$V_{i,\max}/V_{i,\min}$ Bounds of voltage of ith bus.

Variables

$\delta^{\text{CSW}}_{ij,t}$ Binary variable of ijth line, equals 1 if bus j is a parent of bus i else equals 0.
$\gamma^{\text{CH}}_{i,t}/\gamma^{\text{DIS}}_{i,t}$ Charging/discharging state of the ith BESS.
$\gamma^{\text{SCB,UP}}_{i,t}/\gamma^{\text{SCB,DN}}_{i,t}$ Up/down status of ith SCB.
$\gamma^{\text{SL,UP}}_{i,t}/\gamma^{\text{SL,DN}}_{i,t}$ Up/down position of ith SL.
$\gamma^{\text{CSW,UP}}_{ij,t}/\gamma^{\text{CSW,DN}}_{ij,t}$ Up/down position of ith CSW.
$\rho^{\text{SCB}}_{i,t}$ Step status of ith SCB.
$\zeta^{\text{CSW}}_{l,t}$ Binary variable of ijth line, is equal to 1 if the line is linked else equal to 0.
$P^{\text{CL}}_{i,t,\omega}/Q^{\text{CL}}_{i,t,\omega}$ Active/reactive power injection from ith CL.
$P^{\text{SS}}_{i,t,\omega}/Q^{\text{SS}}_{i,t,\omega}$ Active/reactive powers of substation.
$P^{\text{BS}}_{i,t}/Q^{\text{BS}}_{i,t}/E^{\text{BS}}_{i,t}$ Active/reactive power injection and energy state of ith BESS.
$P^{\text{CH}}_{i,t}/P^{\text{DIS}}_{i,t}$ Charge/discharge active power of ith BESS.
$P^{\text{SL,UP}}_{i,t}/P^{\text{SL,DN}}_{i,t}$ Up/down status of active power from ith SL.
$P^{\text{SL}}_{i,t}/Q^{\text{SL}}_{i,t}$ Active/reactive power injection from ith SL.
$P_{ij,t,\omega}/Q_{ij,t,\omega}$ Active/reactive power of ijth line.
$Q^{\text{SCB}}_{i,t}$ Reactive power of ith SCB.
$Q^{\text{SL,UP}}_{i,t}/Q^{\text{SL,DN}}_{i,t}$ Up/down status of reactive power from ith SL.
$V_{i,t,\omega}/\theta_{i,t,\omega}$ Voltage magnitude/Phase angle of ith bus in the system.

I. Introduction

POWER distribution networks across the globe are being transformed from passive to active networks adapting the concept of smart grid. This transformation includes the integration of active elements with diverse characteristics within the existing distribution networks. Some notable active elements are distributed generators (DGs), battery energy storage systems (BESSs), switchable capacitor banks (SCBs), schedulable loads (SLs), curtailable loads (CLs), and controllable switches (CSWs) [1]. To realize the concept of a smart distribution grid (SDG), these active elements are linked to an intelligent distribution management system (DMS) through advanced integrated information and communication technology [1]. To achieve a secure and efficient operation of SDGs, the distribution network operator (DNO) performs day-ahead scheduling (DAS) to determine the dispatch strategies for integrated active elements as a part of DMS. Despite offering several benefits to both utilities and consumers, the DAS of SDGs becomes more intricate due to the simultaneous interaction of multiple issues, such as technological advancements, diversity of active elements, augmentation of new and flexible programs/policies, and intermittent generation from renewable DGs [2]. An extensive amount of work on the DAS of SDGs has been reported in the literature, which is categorized on the basis of problem formulation, consideration of the uncertainties, employment of active elements, constituents of the objective function, and solution techniques.

The problem of DAS of SDGs has been formulated as the nonlinear programming (NLP) problem [1], [15], [17], [18], mixed-integer nonlinear programming (MINLP) problem [5], [6], mixed-integer linear programming (MILP) problem [3], [10], [12], [16], [19], [20], and mixed-integer second-order cone programming (MISOCP) problem [4], [7], [8], [13], [21], [22], [23]. Among various formulations, NLP and MINLP problem formulations are nonconvex, and hence, do not have a theoretical guarantee of global solution [24]. To deal with the nonconvexity of problem formulation, the linear approximation of the power flow has been used to make the DAS formulation as a convex MILP problem [3], [10], [12], [16], [19], [20]. However, linear approximation does not account for the exact line losses, and hence, provides an approximate solution. On the other hand, it has been proven that second-order cone programming (SOCP) relaxations always lead to a global optimum if the conic inequality constraint is exact [24]. Further, for the radial configuration of SDG, the conic constraints are always exact [24]. By imposing additional variables, the SOCP-based power flow can also be linearized without compromising accuracy. However, due to additional variables, the linear SOCP formulation requires more computational time [25].

Another important aspect of the DAS of SDGs is the consideration of the uncertainties associated with electricity price, load demand, and renewable generation. Therefore, to deal with uncertainties in the DAS framework, robust optimization model [8], stochastic programming model [4], [5], [7], [9], and hybrid stochastic/robust optimization model [10], [23] have been developed. The estimation of the uncertainty interval for a robust optimization model is itself a challenging task [26]. On the other hand, the stochastic programming models impose many variables and constraints into the optimization problem and hence, are difficult to solve, particularly for large systems, with available commercial solvers [27], [28].

Among various active elements, BESS has been considered in all the reported works dealing with the DAS of SDGs. However, only in [4], [7], [16], and [20], the reactive power from BESS has been taken into account. Apart from BESS, SCB has been considered in [4], [7], [8], and [9]. The concept of demand response (DR) under DAS framework has been explored in [5], [11], [12], and [29]. However, the coverage of DR in [11], [12], and [29] is restricted only to house level. The nonlinear constraints related to SDG in [5] do not converge to a global solution. In [1], [3], [15], [16], [23], [30], and [31], the network reconfiguration (NR) has also been considered in the DAS formulation. Being a highly combinatorial problem, the NR requires a large amount of computational time and resources to solve [32].

Among the components of the objective function of DAS formulation, the cost of energy from the main grid has been a common component. In addition to grid energy cost, the works presented in [3], [5], [6], [7], [13], [14], [15], and [23] include active element management (AEM) costs in the objective function. The AEM cost reflects the expenses related

TABLE I
TAXONOMY OF THE LITERATURE SURVEY

Ref.	BESS	SCB	SL	CL	NR	Formulation	Uncertainty	AEM Costs	Solver/Technique
[3]/ [4]	✓	X/✓	X	X	✓/X	MILP/MISOCP	X/✓	✓/X	GAMS-CPLEX
[5]/ [6]	✓	X	✓/X	X	X	MINLP	✓	✓	KNITRO/NAA
[7]/ [8]	✓	✓	X	X	X	MISOCP	✓	✓/X	GAMS/MATLAB
[9]/ [10]	✓	✓/X	X	✓/X	X	MISOCP/MILP	✓	X	GUROBI/CPLEX
[11]/ [12]	✓	X	✓	✓	X	NLP/MILP	✓	X	Diagonalization/CPLEX
[13]/ [14]	✓	X	X/✓	X	X	MISOCP	X	✓	YALMIP-GUROBI
[15]/ [16]	✓	X	X	✓/X	✓	NLP/MILP	✓/X	✓/X	SAMCSA/GAMS
Proposed	✓	✓	✓	✓	✓	MISOCP	✓	✓	Benders decomposition (GAMS-CPLEX)

to the operation and maintenance of various active elements. While considering the AEM cost of BESSs, the cost associated with their charging/discharging losses is not considered in the model.

To solve the formulation for DAS for SDGs, a number of techniques/commercial solvers have been used such as genetic algorithm (GA) [1], self-adaptive modified crow search algorithm (SAMCSA) [15], chaotic binary particle swarm optimization [18], natural aggression algorithm (NAA) [6], GAMS-KNITRO [5], GAMS-CPLEX [3], [4], [10], Python-CPLEX [12], GAMS-GUROBI [7], [9], YALMIP-GUROBI [13], [14], Diagnolization method [11], etc. Among various techniques, meta-heuristic approaches provide a near-global solution and do not guarantee a global solution [33]. Further, depending upon the nature of the problem and its dimensional, the available commercial solvers may also fail to converge [27], [28], [32].

Based on the abovementioned literature review on the DAS of SDG, it is observed that no work is available on the development of a synergistic day-ahead scheduling (SDAS) framework for SDGs. Therefore, this article proposes a stochastic SDAS framework for SDGs comprising DGs, BESSs, SCBs, SLs, CLs, and CSWs. A taxonomy is provided in Table I to compare the available literature with the proposed work. The key contributions made through this article are as follows.

1) The developed formulation takes into account DR, NR, active and reactive power contribution from BESSs, and reactive power contribution from SCBs in a synergistic manner, which has not been attempted so far to the best of the authors' knowledge.
2) The developed formulation considers the operational and maintenance costs of BESSs, SCBs, and CSWs; and incentives for SLs and CLs as AEM cost. The cost of charging/discharging losses inside the BESS is also considered here, which has been ignored so far. Thus, closely modeling the operation of an SDG, the proposed SDAS framework gives more realistic figures about operating cost and corresponding benefits to DNOs.
3) The proposed model is formulated as a stochastic optimization problem to consider the uncertainties in renewable generation, load demand, and price of electricity from the main grid. In stochastic optimization problems, the number of decision variables and constraints varies exponentially with the number of scenarios of uncertain parameters [4], [7], [26]. This requires a huge computational burden. Therefore, Monte-Carlo simulation (MCS) followed by a k-means clustering approach [34] is adopted in this article to reduce the computational efforts without compromising much with the accuracy of the solution.
4) The proposed formulation is a convex MISOCP optimization model, which extracts the exact power flow characteristics of SDG and always ensures convergence to a global optimum [24]. However, the stochastic nature of the proposed problem increases its dimension by imposing many additional variables and constraints into it. Also, the consideration of NR under the SDAS framework makes the overall formulation a highly combinatorial problem. Due to these reasons, available commercial solvers either require large computational resources or may not be able to solve the developed formulation [27], [28], [32]. Therefore, to address the limitation of commercial solvers, the proposed formulation is developed as a two-stage SDAS problem. Further, it uses a Benders decomposition-based solution technique to reduce computation time and ensure its convergence.

The proposed framework is tested on a modified IEEE 33-bus distribution network to show its effectiveness in six different cases, applying both deterministic and stochastic approaches. For each case, the results of the proposed MISOCP model have been compared with those of the MILP model [25]. A k means clustering-based scenario reduction technique shows a significant improvement in the computational time and the Benders decomposition-based solution technique ensures the convergence of the proposed model. Also, the results of proposed SDAS scheme are compared with those of similar existing works for validation. The proposed SDAS framework demonstrates a notable improvement in economic and technical performance of SDG. The sensitivity of total operating cost with respect to capacity of active elements is also analyzed.

The rest of this article is organized as follows. Section II overviews the proposed SDAS framework and outlines the uncertainty characterization. The formulation of the scheduling problem is detailed in Section III. The application of Benders decomposition is covered in Section IV. Section V discusses the test system and the analysis of simulation outcomes. Finally, Section VI concludes this article.

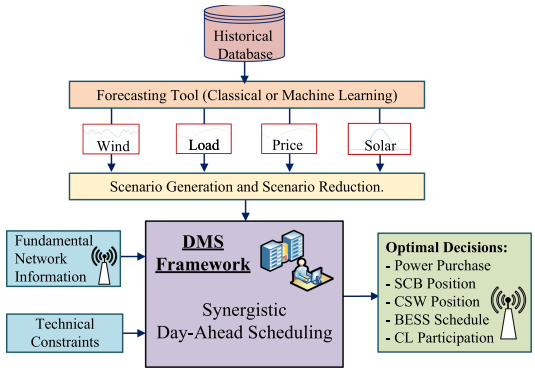

Fig. 1. Proposed synergistic day-ahead scheduling framework.

II. Proposed SDAS and Uncertainty Characterization

A. Proposed SDAS Framework

Assuming that DNO owns and controls all active elements, the concept of the proposed SDAS for the economic operation of the SDG is illustrated in Fig. 1. The photovoltaic generation (PVG) and wind-turbine generation (WTG) are considered as the DGs. The SDAS strives to achieve the best possible day-ahead dispatch of active elements in SDG. Its inputs are forecasts of load demand, electricity price, PVG, and WTG. Numerous conventional regression approaches and data-driven machine learning algorithms are available for forecasting [35], which is outside the focus of this work. In addition to predicting load, generation, and price, the DMS considers the status of its active elements via corresponding distribution remote terminal units, and a range of technical and operational restrictions. The DMS executes SDAS and transmits dispatch schedules to its active ingredients through communication to operate SDGs safely and efficiently.

B. Uncertainty Characterization

In this article, the stochastic variation of forecast of PVG and WTG is assumed to follow a two-parameter Beta probability distribution function (PDF) as [4]

$$f^{\mathrm{g}}_{i,t}(x) = x^{(\alpha^{\mathrm{g}}_{i,t}-1)}\,(1-x)^{(\beta^{\mathrm{g}}_{i,t}-1)} \tag{1}$$

$$\sigma^{\mathrm{g}}_{i,t} = 0.2\left(P^{\mathrm{g}}_{i,t}/P^{\mathrm{CAP}}_{i}\right) + 0.21 = 0.2\mu^{\mathrm{g}}_{i,t} + 0.21 \tag{2}$$

$\mu^{g}_{i,t}$ is the normalized value of $P^{\mathrm{g}}_{i,t}$ with respect to P^{CAP}_{i} and $\sigma^{g}_{i,t}$ can be estimated from (2). Once $\mu^{g}_{i,t}$ and $\sigma^{g}_{i,t}$ are known, the shape parameters of Beta PDF can be estimated from the following relations [4]:

$$\alpha^{\mathrm{g}}_{i,t} = \frac{1}{\left(\sigma^{\mathrm{g}}_{i,t}\right)^2}\left[\left(\mu^{\mathrm{g}}_{i,t}\right)^2 - \left(\mu^{\mathrm{g}}_{i,t}\right)^3\right] - \frac{1}{\mu^{\mathrm{g}}_{i,t}} \tag{3}$$

$$\beta^{\mathrm{g}}_{i,t} = \left(1/\mu^{\mathrm{g}}_{i,t} - 1\right)\alpha^{\mathrm{g}}_{i,t}. \tag{4}$$

Further, the uncertainty in the forecast of load demand and electricity price is assumed to follow a normal PDF with $\mu_{i,t}$ as the mean value and $\sigma_{i,t}$ as the standard deviation of load/price forecast [6]

$$f_{Y_{i,t}}(x) = \frac{1}{\sqrt{2\pi\sigma^2_{i,t}}}\exp\left[-\frac{(x-\mu_{i,t})^2}{2\pi\sigma^2_{i,t}}\right]. \tag{5}$$

To reflect the uncertainty in the proposed SDAS framework, an MCS is conducted using the corresponding PDFs to generate a large number of scenarios for all uncertain parameters. As the number of scenarios in the SDAS model increases, it poses computational challenges making convergence difficult. To address this, a machine learning-based k-means clustering approach [34] is employed in this work to split the given set of scenarios into k clusters based on the Euclidean distance without compromising the quality of the solution.

III. Problem Formulation

A. Objective Function

The proposed SDAS scheme aims to minimize the overall day-ahead operational cost (power purchasing and AEM costs) incurred in SDG. It is formulated as a two-stage stochastic programming problem [36]. In the first stage, the decisions regarding BESS, SCB, SL, and CSW, which must not change before identifying the actual realization of the stochastic process, are taken. In the second stage, the decisions regarding load shedding in CL and power flow, which can vary after identifying the actual realization of the stochastic process, are taken.

$$\min F = F^{\mathrm{SS}} + F^{\mathrm{SCB}} + F^{\mathrm{BS}} + F^{\mathrm{CSW}} + F^{\mathrm{SL}} + F^{\mathrm{CL}} \tag{6}$$

$$F^{\mathrm{SS}} = \sum_{\omega\in\Omega}\tau_\omega \sum_{i\in\Phi^{\mathrm{SS}}}\sum_{t\in T}\left[C^{\mathrm{SS}}_{t,\omega}\,\Delta t\,\left(\,P^{\mathrm{SS}}_{i,t,\omega} + \kappa^{\mathrm{SS}}_{q}Q^{\mathrm{SS}}_{i,t,\omega}\right)\right] \tag{7}$$

$$F^{\mathrm{SCB}} = \sum_{i\in\Phi^{\mathrm{SCB}}}\sum_{t\in T}\left[C^{\mathrm{SCB}}_{i}\left(\gamma^{\mathrm{SCB,UP}}_{i,t} + \gamma^{\mathrm{SCB,DN}}_{i,t}\right)\right] \tag{8}$$

$$F^{\mathrm{BS}} = \sum_{i\in\Phi^{\mathrm{BS}}}\sum_{t\in T}\Delta t\Bigg[C^{\mathrm{BS}}_{i}P^{\mathrm{CH}}_{i,t} + P^{\mathrm{DIS}}_{i,t}\left(C^{\mathrm{BS}}_{i} + \sum_{\omega\in\Omega}\tau_\omega C^{\mathrm{SS}}_{t,\omega}(1-\eta^{\mathrm{DIS}}_{i})\right)\Bigg] \tag{9}$$

$$F^{\mathrm{SL}} = \sum_{i\in\Phi^{\mathrm{SL}}}\sum_{t\in T}\Delta t\left[C^{\mathrm{SL,UP}}_{i}P^{\mathrm{SL,UP}}_{i,t} + C^{\mathrm{SL,DN}}_{i}P^{\mathrm{SL,DN}}_{i,t}\right] \tag{10}$$

$$F^{\mathrm{CL}} = \sum_{\omega\in\Omega}\tau_\omega \sum_{i\in\Phi^{\mathrm{CL}}}\sum_{t\in T}\left[C^{\mathrm{CL}}_{i}\Delta t P^{\mathrm{CL}}_{i,t,\omega}\right] \tag{11}$$

$$F^{\mathrm{CSW}} = \sum_{ij\in\Phi^{\mathrm{CSW}}}\sum_{t\in T}\left[C^{\mathrm{CSW}}_{ij}\left(\gamma^{\mathrm{CSW,UP}}_{ij,t} + \gamma^{\mathrm{CSW,DN}}_{ij,t}\right)\right]. \tag{12}$$

The total day-ahead operational cost of SDG, F, as given in (6), consists of the cost of power purchase from the upper grid and AEM cost. F^{SS} represents the expected cost of active and reactive energy purchased from the upper grid [7]. F^{SCB} and F^{CSW} are the costs associated with the operation and maintenance of SCB and CSW, respectively. F^{BS} represents the costs of

operation and maintenance of BESS including its losses during the discharging [37]. F^{SL} denotes the total incentives paid to SLs for shifting their consumption from one-time interval to another. F^{CL} indicates the expected cost of energy not served to CLs.

B. Constraints

1) Battery Energy Storage System:

$$\gamma_{i,t}^{\mathrm{CH}} + \gamma_{i,t}^{\mathrm{DIS}} \leq 1 \;\; \forall t \; \forall i \in \Phi^{\mathrm{BS}} \tag{13}$$

$$\left.\begin{aligned} P_{i,t}^{\mathrm{BS}} &= P_{i,t}^{\mathrm{DIS}} - P_{i,t}^{\mathrm{CH}} \\ (P_{i,t}^{\mathrm{BS}})^2 + (Q_{i,t}^{\mathrm{BS}})^2 &\leq (S_{i,\max}^{\mathrm{BS}})^2 \end{aligned}\right\} \forall t \; \forall i \in \Phi^{\mathrm{BS}} \tag{14}$$

$$\begin{aligned} E_{i,t+1}^{\mathrm{BS}} = E_{i,t}^{\mathrm{BS}} &+ \Delta t \, \eta_i^{\mathrm{CH}} P_{i,t}^{\mathrm{CH}} \\ &- \Delta t \, \eta_i^{\mathrm{DIS}} P_{i,t}^{\mathrm{DIS}} \qquad \forall t \; \forall i \in \Phi^{\mathrm{BS}} \end{aligned} \tag{15}$$

$$\left.\begin{aligned} 0 \leq P_{i,t}^{\mathrm{CH}} &\leq \gamma_{i,t}^{\mathrm{CH}} S_{i,\max}^{\mathrm{BS}} \\ 0 \leq P_{i,t}^{\mathrm{DIS}} &\leq \gamma_{i,t}^{\mathrm{DIS}} S_{i,\max}^{\mathrm{BS}} \\ E_{i,\min}^{\mathrm{BS}} \leq E_{i,t}^{\mathrm{BS}} &\leq E_{i,\max}^{\mathrm{BS}} \end{aligned}\right\} \forall t \; \forall i \in \Phi^{\mathrm{BS}}. \tag{16}$$

Equation (13) governs the charging or discharging of the BESS within the time interval t. The convex quadratic constraints linked to the active and reactive power of the BESS are expressed by (14). The energy state of BESS is reflected through the utilization of (15). The operational boundaries that the BESS must adhere to are outlined in (16).

2) Switchable Capacitor Bank:

$$\gamma_{i,t}^{\mathrm{SCB,UP}} + \gamma_{i,t}^{\mathrm{SCB,DN}} \leq 1 \;\; \forall t \; \forall i \in \Phi^{\mathrm{SCB}} \tag{17}$$

$$\sum_{t \in T} \left(\gamma_{i,t}^{\mathrm{SCB,UP}} + \gamma_{i,t}^{\mathrm{SCB,DN}} \right) \leq N_{i,\max}^{\mathrm{SCB}} \;\; \forall i \in \Phi^{\mathrm{SCB}} \tag{18}$$

$$\left.\begin{aligned} \rho_{i,t}^{\mathrm{SCB}} - \rho_{i,t-1}^{\mathrm{SCB}} &\leq \gamma_{i,t}^{\mathrm{SCB,UP}} \Psi_{i,\max}^{\mathrm{SCB}} - \gamma_{i,t}^{\mathrm{SCB,DN}} \\ \rho_{i,t}^{\mathrm{SCB}} - \rho_{i,t-1}^{\mathrm{SCB}} &\geq \gamma_{i,t}^{\mathrm{SCB,UP}} - \gamma_{i,t}^{\mathrm{SCB,DN}} \Psi_{i,\max}^{\mathrm{SCB}} \end{aligned}\right\} \forall t \; \forall i \in \Phi^{\mathrm{SCB}} \tag{19}$$

$$Q_{i,t}^{\mathrm{SCB}} = \rho_{i,t}^{\mathrm{SCB}} \cdot Q_{i,\mathrm{step}}^{\mathrm{SCB}} \qquad \forall t \; \forall i \in \Phi^{\mathrm{SCB}}. \tag{20}$$

Equation (17) asserts that at any given time t, an SCB cannot simultaneously increase and decrease reactive power compensation. The cumulative number of SCB switching operations within a day must not surpass the maximum allowable limit, as specified in (18). When incorporating switching variables and the overall bank count, (19) constrains the regulatory range within which the SCB operates. The cumulative reactive power contribution from each SCB is indicated in (20).

3) Demand Response: The DR is mainly categorized as load shifting and load curtailment [11]. The process of shifting a fraction of the consumption of a given consumer from a one-time interval to another time interval based on a bilateral contract with DNO is known as load shifting. Incentives are provided to those customers who participate in the load shifting. Load curtailment is known as the process of curtailing a fraction of the consumers' consumption by paying the cost of energy not served.

a) Shiftable load:

$$\gamma_{i,t}^{\mathrm{SL,UP}} + \gamma_{i,t}^{\mathrm{SL,DN}} \leq 1 \;\; \forall t \; \forall i \in \Phi^{\mathrm{SL}} \tag{21}$$

$$\left.\begin{aligned} 0 \leq P_{i,t}^{\mathrm{SL,UP}} &\leq \gamma_{i,t}^{\mathrm{SL,UP}} \kappa_i^{\mathrm{SL,UP}} P_{i,t}^{\mathrm{LD,FORE}} \\ 0 \leq P_{i,t}^{\mathrm{SL,DN}} &\leq \gamma_{i,t}^{\mathrm{SL,DN}} \kappa_i^{\mathrm{SL,DN}} P_{i,t}^{\mathrm{LD,FORE}} \\ P_{i,t}^{\mathrm{SL}} &= P_{i,t}^{\mathrm{SL,DN}} - P_{i,t}^{\mathrm{SL,UP}} \\ Q_{i,t}^{\mathrm{SL,UP}} &= \tan(\Theta_{i,t}^{\mathrm{SL}}) P_{i,t}^{\mathrm{SL,UP}} \\ Q_{i,t}^{\mathrm{SL,DN}} &= \tan(\Theta_{i,t}^{\mathrm{SL}}) P_{i,t}^{\mathrm{SL,DN}} \\ Q_{i,t}^{\mathrm{SL}} &= Q_{i,t}^{\mathrm{SL,DN}} - Q_{i,t}^{\mathrm{SL,UP}} \end{aligned}\right\} \forall t \; \forall i \in \Phi^{\mathrm{SL}} \tag{22}$$

$$\left.\begin{aligned} \textstyle\sum_{t \in T} \left(P_{i,t}^{\mathrm{SL,UP}} - P_{i,t}^{\mathrm{SL,DN}} \right) &= 0 \\ \textstyle\sum_{t \in T} \left(Q_{i,t}^{\mathrm{SL,UP}} - Q_{i,t}^{\mathrm{SL,DN}} \right) &= 0 \end{aligned}\right\} \forall t \; \forall i \in \Phi^{\mathrm{SL}}. \tag{23}$$

The increase or decrease in SL consumption cannot occur simultaneously during a given time interval t as given in (21). The limits on increase or decrease in consumption of SL are expressed in (22). Equation (23) ensures that the total increase in consumption of SL should be equal to the total decrease in consumption of SL over a day, i.e., there is no loss of energy served to SL.

b) Curtailable load:

$$\left.\begin{aligned} 0 \leq P_{i,t,\omega}^{\mathrm{CL}} &\leq P_{i,t,\omega}^{\mathrm{LD}} \\ 0 \leq Q_{i,t,\omega}^{\mathrm{CL}} &\leq Q_{i,t,\omega}^{\mathrm{LD}} \end{aligned}\right\} \forall i \in \Phi^{\mathrm{CL}} \; \forall t \; \forall \omega. \tag{24}$$

The bounds on active and reactive power of CLs are provided in (24), ensuring constant power factor operation.

4) Network Reconfiguration and SOCP-Based Power Flow:

$$\delta_{ij,t}^{\mathrm{CSW}} + \delta_{ji,t}^{\mathrm{CSW}} = \zeta_{l,t}^{\mathrm{CSW}} \;\; \forall t \; \forall l \tag{25}$$

$$\sum_{j \in i} \delta_{ij,t}^{\mathrm{CSW}} = 1 \;\; \forall t \; \forall i \in \Phi^{\mathrm{LD}} \tag{26}$$

$$\sum_{j \in i} \delta_{ij,t}^{\mathrm{CSW}} = 0 \;\; \forall t \; \forall i \in \Phi^{\mathrm{SS}} \tag{27}$$

$$\gamma_{ij,t}^{\mathrm{CSW,UP}} + \gamma_{ij,t}^{\mathrm{CSW,DN}} \leq 1 \;\; \forall t \; \forall ij \tag{28}$$

$$\zeta_{l,t}^{\mathrm{CSW}} - \zeta_{l,t-1}^{\mathrm{CSW}} = \gamma_{ij,t}^{\mathrm{CSW,UP}} - \gamma_{ij,t}^{\mathrm{CSW,DN}} \;\; \forall t \; \forall ij \tag{29}$$

$$\sum_{t \in T} \left(\gamma_{ij,t}^{\mathrm{CSW,UP}} + \gamma_{ij,t}^{\mathrm{CSW,DN}} \right) \leq N_{ij,\max}^{\mathrm{CSW}} \;\; \forall t \; \forall ij \tag{30}$$

$$U_{i,t,\omega} = V_{i,t,\omega}^2 / \sqrt{2} \; \forall t \; \forall i \; \forall \omega \tag{31}$$

$$\left.\begin{aligned} W_{ij,t,\omega}^{\mathrm{R}} &= W_{ji,t,\omega}^{\mathrm{R}} = V_{i,t,\omega} V_{j,t,\omega} \cos(\theta_{ij,t,\omega}) \\ W_{ij,t,\omega}^{\mathrm{I}} &= -W_{ji,t,\omega}^{\mathrm{I}} = V_{i,t,\omega} V_{j,t,\omega} \sin(\theta_{ij,t,\omega}) \end{aligned}\right\} \forall t \; \forall ij \; \forall \omega \tag{32}$$

$$2U_{i,t,\omega}^{l} U_{j,t,\omega}^{l} \geq (W_{ij,t,\omega}^{\mathrm{R}})^2 + (W_{ij,t,\omega}^{\mathrm{I}})^2 \;\; \forall t \; \forall ij \; \forall \omega \tag{33}$$

$$\left.\begin{aligned} 0 \leq U_{i,t,\omega}^{l} &\leq \left(V_{i,\max}^2 / \sqrt{2} \right) \zeta_{l,t}^{\mathrm{CSW}} \\ 0 \leq U_{j,t,\omega}^{l} &\leq \left(V_{j,\max}^2 / \sqrt{2} \right) \zeta_{l,t}^{\mathrm{CSW}} \end{aligned}\right\} \forall t \; \forall l \; \forall \omega \tag{34}$$

$$\left.\begin{aligned} 0 \leq U_{i,t,\omega} - U_{i,t,\omega}^{l} &\leq \left[V_{i,\max}^2 \left(1 - \zeta_{l,t}^{\mathrm{CSW}} \right) \right] / \sqrt{2} \\ 0 \leq U_{j,t,\omega} - U_{j,t,\omega}^{l} &\leq \left[V_{j,\max}^2 \left(1 - \zeta_{l,t}^{\mathrm{CSW}} \right) \right] / \sqrt{2} \end{aligned}\right\} \forall t \; \forall l \; \forall \omega \tag{35}$$

$$\left.\begin{aligned} P_{ij,t,\omega} &= \sqrt{2} g_{ij} U^{l}_{i,t,\omega} - g_{ij} W^{\mathrm{R}}_{ij,t,\omega} - b_{ij} W^{\mathrm{I}}_{ij,t,\omega} \\ Q_{ij,t,\omega} &= -\sqrt{2} b_{ij} U^{l}_{i,t,\omega} + b_{ij} W^{\mathrm{R}}_{ij,t,\omega} - g_{ij} W^{\mathrm{I}}_{ij,t,\omega} \\ &\qquad \forall t\ \forall ij\ \forall \omega \end{aligned}\right\} \tag{36}$$

$$P_{ij,t,\omega}, Q_{ij,t,\omega} \begin{cases} \neq 0, & \text{if } \zeta^{\mathrm{CSW}}_{l,t} = 1 \\ = 0, & \text{if } \zeta^{\mathrm{CSW}}_{l,t} = 0 \end{cases} \tag{37}$$

$$\left.\begin{aligned} &P^{\mathrm{SS}}_{i,t,\omega} + P^{\mathrm{BS}}_{i,t} + P^{\mathrm{CL}}_{i,t,\omega} + P^{\mathrm{SL}}_{i,t} + \\ &P^{\mathrm{WT}}_{i,t,\omega} + P^{\mathrm{PV}}_{i,t,\omega} - P^{\mathrm{LD}}_{i,t,\omega} = \textstyle\sum_{j\in\Phi^i} P_{ij,t,\omega} \\ &Q^{\mathrm{SS}}_{i,t,\omega} + Q^{\mathrm{BS}}_{i,t} + Q^{\mathrm{CL}}_{i,t,\omega} + Q^{\mathrm{SL}}_{i,t} + \\ &Q^{\mathrm{SCB}}_{i,t} - Q^{\mathrm{LD}}_{i,t,\omega} = \textstyle\sum_{j\in\Phi^i} Q_{ij,t,\omega} \end{aligned}\right\} \forall t\ \forall i\ \forall \omega \tag{38}$$

$$\begin{aligned} I^2_{ij,t,\omega} &= \sqrt{2}\left(g^2_{ij} + b^2_{ij}\right)\left(U^{l}_{i,t,\omega} + U^{l}_{j,t,\omega} - 2W^{\mathrm{R}}_{ij,t,\omega}\right) \\ &\leq I^2_{ij,\max}\ \ \forall t\ \forall ij\ \forall \omega \end{aligned} \tag{39}$$

$$\left.\begin{aligned} &U_{i,t,\omega} = 1/\sqrt{2}\ \ \forall i \in \Phi^{\mathrm{SS}} \\ &V^2_{i,\min}/\sqrt{2} \leq U_{i,t,\omega} \leq V^2_{i,\max}/\sqrt{2}\ \ \forall i \in \Phi^{\mathrm{LD}} \end{aligned}\right\} \forall t\ \forall \omega \tag{40}$$

$$\left.\begin{aligned} &-P_{ij,\max} \leq P_{ij,t,\omega} \leq P_{ij,\max} \\ &-Q_{ij,\max} \leq Q_{ij,t,\omega} \leq Q_{ij,\max} \\ &0 \leq W^{\mathrm{R}}_{ij,t,\omega} \leq V_{i,\max} V_{j,\max} \\ &-V_{i,\max} V_{j,\max} \leq W^{\mathrm{I}}_{ij,t,\omega} \leq V_{i,\max} V_{j,\max} \end{aligned}\right\} \forall t\ \forall ij\ \forall \omega \tag{41}$$

$$\left.\begin{aligned} &P^{\mathrm{SS}}_{i,\min} \leq P^{\mathrm{SS}}_{i,t,\omega} \leq P^{\mathrm{SS}}_{i,\max} \\ &Q^{\mathrm{SS}}_{i,\min} \leq Q^{\mathrm{SS}}_{i,t,\omega} \leq Q^{\mathrm{SS}}_{i,\max} \end{aligned}\right\} \forall t\ \forall i \in \Phi^{\mathrm{SS}}\ \forall \omega. \tag{42}$$

Equations (25)–(27) represent the spanning tree constraints, which ensure the radial structure of the network [25]. Equations (28)–(29) represent the time coupling relationship between spanning tree variables. The maximum daily count of switching actions on CSWs is constrained by (30). Equations (31)–(33) provide the expressions and definitions of newly introduced variables associated with SOCP [25]. The connection between NR and variables of power flow is given in (34)–(35). Here, the new variables $(U^{l}_{i,t,\omega}, U^{l}_{j,t,\omega})$ are denoted for each separate line. These variables are set to zero, when $\zeta^{\mathrm{CSW}}_{l,t} = 0$, and greater than zero, when $\zeta^{\mathrm{CSW}}_{l,t} = 1$. The linear expressions for the active and reactive power flow on line ij for time interval t are provided in (36), where $g_{ij} + jb_{ij} = 1/(r_{ij} + jx_{ij})$. The presence of the line in the network is verified in (37). Power balance expression for SDG and its connected components are specified in (38). The square of the line current limit is linearly represented in (39). Bounds on power flow variables are defined by (40)–(42).

IV. Solution Technique: Benders Decomposition for SDAS Scheme

A significant challenge in solving the proposed stochastic MISOCP-based SDAS model stems from the abundance of conic ac power flow constraints associated with stochastic scenarios. The combinatorial nature of the NR problem further increases the complexity of proposed SDAS scheme while solving it. Commercial solvers typically struggle to handle such large-scale stochastic MILP or MISOCP problems. In such cases, Benders decomposition could be useful to obtain the solution [28]. It partitions the initial problem into a master problem and multiple subproblems, which are solved iteratively to achieve the optimal solution. A generalized Benders decomposition is presented in [38], which theoretically proves that it reaches an optimal solution for mixed-integer conic problems. A bilinear Benders decomposition has been exploited to solve a stochastic and chance-constrained MISOCP model for expansion planning of the distribution network in [27]. Motivated by its practicality in solving large-scale stochastic MISOCP problems, the Benders decomposition used in [27] is adopted to solve the proposed SDAS.

A. Compact Form of Proposed SDAS Framework

Let x_t be the variables corresponding to the first stage (day-ahead) with related parameter matrices $(c_t, F_t, f, M_t, m, A_t)$. Further, let $y_{t,\omega}$ be the variables corresponding to the second stage (operation) in scenario ω with related parameter matrices $(g_{t,\omega}, E_{t,\omega}, d_{t,\omega}, B_{t,\omega}, l_{t,\omega}, H_{t,\omega}, h_{t,\omega})$. Here, the matching dual variables of each constraint in the operation stage are denoted by a colon.

$$\begin{aligned} x_t = [&P^{\mathrm{CH}}_{i,t}, P^{\mathrm{DIS}}_{i,t}, \gamma^{\mathrm{CH}}_{i,t}, \gamma^{\mathrm{DIS}}_{i,t}, P^{\mathrm{BS}}_{i,t}, Q^{\mathrm{BS}}_{i,t}, E^{\mathrm{BS}}_{i,t}, \gamma^{\mathrm{SCB,UP}}_{i,t}, \\ &\gamma^{\mathrm{SCB,DN}}_{i,t}, \rho^{\mathrm{SCB}}_{i,t}, Q^{\mathrm{SCB}}_{i,t}, \gamma^{\mathrm{SL,UP}}_{i,t}, \gamma^{\mathrm{SL,DN}}_{i,t}, P^{\mathrm{SL,UP}}_{i,t}, P^{\mathrm{SL,DN}}_{i,t}, P^{\mathrm{SL}}_{i,t}, \\ &Q^{\mathrm{SL,UP}}_{i,t}, Q^{\mathrm{SL,DN}}_{i,t}, Q^{\mathrm{SL}}_{i,t}, \delta^{\mathrm{CSW}}_{ij,t}, \zeta^{\mathrm{CSW}}_{ij,t}, \gamma^{\mathrm{CSW,UP}}_{ij,t}, \gamma^{\mathrm{CSW,DN}}_{ji,t}] \end{aligned}$$

$$\begin{aligned} y_{t,\omega} = [&U_{i,t,\omega}, W^{\mathrm{R}}_{ij,t,\omega}, W^{\mathrm{I}}_{ij,t,\omega}, U^{ij}_{i,t,\omega}, U^{ij}_{j,t,\omega}, P_{ij,t,\omega}, \\ &Q_{ij,t,\omega}, P^{\mathrm{SS}}_{i,t,\omega}, Q^{\mathrm{SS}}_{i,t,\omega}, P^{\mathrm{CL}}_{i,t,\omega}, Q^{\mathrm{CL}}_{i,t,\omega}] \end{aligned}$$

$$\min_{\{x_t\},\{y_{t,\omega}\}} \ \sum_{t\in T}(c_t x_t) + \sum_{t\in T}\sum_{\omega\in\Omega}(\tau_\omega g_{t,\omega} y_{t,\omega}) \tag{43}$$

$$\text{s.t.}\ \ F_t x_t \leq f_t \ \ \forall t \tag{44}$$

$$\sum_{t\in T}(M_t x_t) \leq m \tag{45}$$

$$E_{t,\omega} y_{t,\omega} = d_{t,\omega} \qquad : \lambda_{t,\omega}\ \ \forall t\ \forall \omega \tag{46}$$

$$A_t x_t + B_{t,\omega} y_{t,\omega} \geq l_{t,\omega} \qquad : \xi_{t,\omega}\ \ \forall t\ \forall \omega \tag{47}$$

$$||H_{t,\omega} y_{t,\omega}|| \leq h_{t,\omega} y_{t,\omega} \qquad : (\mu_{t,\omega}, \sigma_{t,\omega})\ \ \forall t\ \forall \omega. \tag{48}$$

The objective function including the first and second stage costs is represented in (43). The constraints related to day-ahead decision variables are described in (44)–(45); nodal power balance equations are represented in (46); constraints linking day-ahead and operation variables are described in (47); and conic constraints are represented in (48).

B. Subproblem and Master Problem

In this context, the subproblem takes the form of the dual representation of the second-stage recourse problem within scenario ω, given a specific $\hat{x_t}^k$ derived from the k^{th} iteration. The optimum objective achieved in the subproblem is employed to establish an upper limit for the main problem. Within the second-stage recourse problem, load curtailment is taken into account but is subjected to a penalty within the objective function. Consequently, this approach guarantees the strict feasibility of the second-stage recourse problem, thereby ensuring the strong

Algorithm 1: Benders Decomposition for MISOCP-Based Stochastic SDAS.

Input: Network data, scenarios (load, PVG, WTG, and price),
parameters corresponding to all active elements.

Initialization : $LB = -\infty$ and $UB = \infty$

for $k \in K$ **do**
  Solve MP: obtain $\hat{x}^k$ & V^k
  Update $LB = V^k$
  for $\omega \in \Omega$ **do**
    Solve SP_ω: obtain $\hat{J}_\omega$
  end for
  Update $UB = \min\{UB, \quad c\hat{x}^k + \rho \sum_{\omega\in\Omega} \tau_\omega \hat{J}_\omega\}$
  if $(|\frac{UB-LB}{LB}| \leq \varepsilon)$ **then**
    Stop
  end if
end for

Output: Optimal solution ($\hat{F}$), which is related with UB.

duality of the MISOCP problem.

$$SP_\omega : J_\omega = \max \quad \sum_{t\in T} \left[\xi_{t,\omega}\left(l_{t,\omega} - A_t \hat{x_t}^k\right) + \lambda_{t,\omega} d_{t,\omega}\right] \quad (49)$$

$$\text{s.t. } E_{t,\omega}\lambda_{t,\omega} + B_{t,\omega}\xi_{t,\omega} + H_{t,\omega}\sigma_{t,\omega} + \mu_{t,\omega}h_{t,\omega} = g_{t,\omega} \quad \forall t \ \forall\omega \quad (50)$$

$$||\sigma_{t,\omega}|| \leq \mu_{t,\omega} \quad \forall t \ \forall\omega \quad (51)$$

$$\theta_{t,\omega}, \mu_{t,\omega} \geq 0, \quad \lambda_{t,\omega}, \sigma_{t,\omega} \ \text{ unbound.} \quad (52)$$

Let $(\hat{\theta}_{t,\omega}, \hat{\lambda}_{t,\omega}, \hat{\mu}_{t,\omega}, \hat{\sigma}_{t,\omega})$ be the optimal solution obtained from SP_ω. Next, the master problem for tth iteration is considered. Bender cuts are the linear function of optimal value from SP_ω in the proposed model.

$$MP : \min \quad \sum_{t\in T} c_t x_t + \rho \sum_{\omega\in\Omega} \tau_\omega \eta_\omega \quad (53)$$

$$\text{s.t. } F_t x_t \leq f_t \quad \forall t \quad (54)$$

$$\sum_{t\in T} (M_t x_t) \leq m \quad (55)$$

$$\sum_{t\in T} \left[\hat{\xi}^\nu_{t,\omega}\left(l_{t,\omega} - A_t x_t\right) + \hat{\lambda}^\nu_{t,\omega} d_{t,\omega}\right] \leq \eta_\omega, \ 1 \leq \nu \leq k \ \forall\omega. \quad (56)$$

C. Solution Algorithm

The complete methodology for addressing the two-stage stochastic MISOCP challenge is outlined in Algorithm 1. Here, the current lower and upper boundaries are denoted as LB and UB, respectively, with ε representing the optimality criterion and K representing a set of iterations.

V. Case Study

The proposed SDAS scheme is executed on an Intel(R) Core(TM) i7-8700 CPU, 3.20 GHz, and 16 GB RAM Windows-based personal computer and solved using GAMS software with the CPLEX solver under default settings. Unless otherwise stated, the maximum simulation time (T) is 7,200 s. The optimality tolerance is set to the default value in GAMS ($\epsilon = 0.01\ \%$).

TABLE II
Details of Active Elements in IEEE 33-Bus System

Element	Location	Details/Specifications
PVG	8, 20, 25, 30.	0.6 MW.
WTG	18, 33.	0.6 MW.
SCB	6, 14, 17, 21, 24, 28.	$Q^{\text{SCB}}_{i,\text{step}} = 0.05$ MVAr, $\Psi^{\text{SCB}}_{i,\text{max}} = 5$, $N^{\text{SCB}}_{i,\text{max}} = 5$, $C^{\text{SCB}}_i = 0.5\$$.
BESS	5, 15, 26, 32.	$S^{\text{BS}}_{i,\text{max}} = 0.2$ MVA, $E^{\text{BS}}_{i,\text{max}} = 0.45$ MWh, $E^{\text{BS}}_{i,\text{min}} = 0.05$ MWh, $\eta^{\text{CH}}_i = 1/\eta^{\text{DIS}}_i = 0.95$, $C^{\text{BS}}_i = 5\$$/MW.
SL	3, 4, 7, 13, 14, 19, 20, 24, 25, 28.	$\kappa^{\text{SL,DN}}_i = \kappa^{\text{SL,UP}}_i = 0.2$, $C^{\text{SL,UP}}_i = C^{\text{SL,DN}}_i = 5\$$/MW.
CL	All buses	$C^{\text{CL}}_i = 5,000\ \$$/MW.
CSW	5, 10, 15, 20, 22, 28, 31, 33, 34, 35, 36, 37.	$C^{\text{CSW}}_{ij} = 1$, $N^{\text{CSW}}_{ij,\text{max}} = 5$.

TABLE III
Classification of Cases

Case	SCB	BESS	SL	CL	CSW
I	X	X	X	X	X
II	✓	✓	X	X	X
III	✓	X	✓	✓	X
IV	✓	✓	✓	✓	X
V	X	X	X	X	✓
VI	✓	✓	✓	✓	✓

The proposed SDAS scheme is tested on an IEEE 33-bus test distribution network after adding active elements to the standard network [8]. The essential data related to the 33-bus test network is obtained from [8]. The data corresponding to different active elements are provided in Table II. Initially, the CSWs of lines 33-37 are OFF, and the remaining CSWs are ON. The day-ahead forecasts of load and electricity price have been obtained from [10]. Similarly, the day-ahead forecasts of PVG and WTG have been assumed as generation profiles, which are taken from [39]. The reactive counterpart, k^{SS}_q of upper grid price, is 0.05 [1]. The lower and upper and limits on active/reactive power from substation (SS) are 0 and 6 MW/MVAr, respectively. The minimum and maximum voltage limits at each bus are 0.9 pu and 1.1 pu, respectively.

The proposed SDAS scheme is applied to the test system in six cases, considering different combinations of active elements as presented in Table III. For each case, the proposed SDAS formulation is solved using deterministic as well as stochastic approaches. In deterministic scheduling, the forecast values are assumed to be accurate without any error. In stochastic SDAS, the uncertainties associated with the forecasts of load, electricity price, and PVG and WTG are accounted for as discussed in Part B of Section II. The standard deviation of the load and price forecast is assumed as 5%. A total of 10,000 scenarios have been generated using MCS utilizing corresponding PDFs of uncertain variables. The proposed stochastic MISOCP problem for Case-IV with 10,000 scenarios converges in approximately

Fig. 2. Error in the objective function and computational time with a different number of clusters.

TABLE IV
RESULTS ON 33-BUS SYSTEM WITH DETERMINISTIC SDAS

Case	MISOCP Model: Operational cost ($)	MISOCP Model: Time (sec.) / Gap (%)	MILP Model: Operational cost ($)	MILP Model: Time (sec.) / Gap (%)
Without Benders decomposition				
I	5,766.57	3.34 / ϵ	5,763.99	33.78 / ϵ
II	5,226.96	18.15 / ϵ	5,224.39	135.98 / ϵ
III	5,180.85	15.24 / ϵ	5,178.63	97.62 / ϵ
IV	4,997.37	31.82 / ϵ	4,995.81	171.52 / ϵ
V	5,748.52	T / 0.91	5,738.54	T / 0.59
VI	5,002.63	T / 0.53	4,989.45	T / 0.32
With Benders decomposition				
V	5,725.26	748.89 / ϵ	5,723.60	1,536.03 / ϵ
VI	4,965.97	1,371.78 / ϵ	4,963.07	2,579.41 / ϵ

75 h with an expected cost of $4,999.68, which is impractical for DAS of a SDG, as the DAS decisions are to be taken on daily basis. Therefore, for faster convergence, a k-means clustering algorithm [34] has been used to shrink these 10,000 scenarios. A larger number of clusters increases the computational complexity, while a smaller number of clusters compromises the uncertainty representation [40]. Therefore, to reach an optimum number of clusters, the experiment has been conducted by varying the number of clusters from 5 to 50 in Case-IV and observing the results in terms of the error in the objective function and associated computational burden as shown in Fig. 2. For the computation of error in the objective function, the results obtained by MCS is taken as the reference. From this figure, it is observed that the scenario reduction approach significantly saves computational time without much affecting the accuracy of results. The scenario reduction using 25 clusters gives a tradeoff between accuracy in the results as well as computational time. Hence, in this article, 25 clusters have been used for further analysis.

The results of deterministic and stochastic SDAS are given in Table IV and Table V, respectively. Due to inclusion of uncertainty, the total operational cost by stochastic SDAS is always less than that by deterministic SDAS and the computational time by stochastic SDAS is always more than that by deterministic SDAS. However, the results by deterministic and stochastic SDAS exhibit a similar variation with respect to the different cases. Further, in these tables, the results of proposed MISOCP model have been compared with those by MILP model for each case. To obtain the MILP model, the conic constraint (51) is linearized using the polyhedral approximation of feasible convex region [25]. Though both models result in the approximate same value of total operational cost with deterministic

TABLE V
RESULTS ON 33-BUS SYSTEM WITH STOCHASTIC SDAS

Case	MISOCP Model: Operational cost ($)	MISOCP Model: Time (sec.) / Gap (%)	MILP Model: Operational cost ($)	MILP Model: Time (sec.) / Gap (%)
Without Benders decomposition				
I	5,664.32	37.81 / ϵ	5,661.56	332.67 / ϵ
II	5,130.35	2,746.71 / ϵ	5,127.89	4,324.61 / ϵ
III	5,128.42	2,167.45 / ϵ	5,125.58	5,096.27 / ϵ
IV	4,921.18	3,468.91 / ϵ	4,919.41	6,156.83 / ϵ
V	–	T / (N/A)	–	T / (N/A)
VI	–	T / (N/A)	–	T / (N/A)
With Benders decomposition				
V	5,562.92	2,264.67 / ϵ	5,560.12	4,426.58 / ϵ
VI	4,834.66	3,378.13 / ϵ	4,830.98	5,978.56 / ϵ

as well as stochastic approaches, their computational efforts are significantly different. This is because each conic constraint containing 4 variables in the MISOCP model is linearized using 6 constraints containing 24 variables in the MILP model [25]. Thus, the proposed MISOCP model is found to be computationally efficient than its MILP counterpart.

A. Effectiveness of Benders Decomposition

For both MISOCP and MILP models under deterministic as well as stochastic SDAS, different cases have been first solved without Benders decomposition. It is observed from Tables IV and V that the solver is unable to converge for Case-V and Case-VI within T. The reason behind this is the introduction of extra variables in the SDAS problem due to the combinatorial nature of the NR. Interestingly, the total number of variables becomes 13,104 (binary: 4,272, integer: 144, continuous: 8,688) and 172,080 (binary: 4,272, integer: 144, continuous: 167,664) in deterministic and stochastic SDAS, respectively. For these two cases, the problem converges to an optimum value within T only when Benders decomposition is used. With Benders decomposition, the deterministic MISOCP model for Cases-V and VI converges within 748.89 s and 1,371.78 s, respectively. Similarly, the stochastic MISOCP model for Cases-V and VI converges within 2,264.67 s and 3,378.13 , respectively, with Benders decomposition. For the MILP model also, Benders decomposition is able to converge to an optimum value within T. Thus, Benders decomposition helps to solve the proposed large-scale SDAS.

B. Validation of Proposed SDAS Scheme

To validate the effectiveness of the proposed SDAS scheme, the results obtained by it have been compared with those by some of the existing methods reported in the literature. While implementing other methods, the same problem formulations, same active elements, and same way of handling the uncertainty have been considered as reported in those methods (Refer Table I). For the sake of comparison, a common 33-bus test network has been used for all the methods. The diesel generators used in the works [16] and [21], are not considered here for the purpose of comparison. A comparison of results in terms of total operating cost, daily energy losses, peak demand on SS, and minimum

TABLE VI
COMPARATIVE STUDY WITH EXISTING WORKS

Ref.	Operational cost, F ($)	Losses (MWh)	Peak demand on SS (MVA)	Minimum voltage (pu)
[21]	5,296.05	1.6369	4.0121	0.9384
[16]	5,161.92	1.3480	4.4075	0.9184
[4]	5,145.67	1.5137	4.6281	0.9337
[6]	5,249.24	2.9666	5.6932	0.9029
[30]	5,568.70	2.3546	5.4389	0.9193
Proposed	4,834.66	1.2265	4.5453	0.9423

voltage in the network is shown in Table VI. It is observed from this table that among different methods, the proposed scheme results minimum operating cost, minimum daily energy losses, and maximum improvement in minimum voltage. Also, among different stochastic formulations [4], [6], [30], the proposed scheme results minimum peak demand on SS. This is due to the consideration of diverse active elements in the proposed SDAS scheme. Thus, the results presented in Table VI validate the effectiveness of the proposed method over other methods.

C. Analysis With Proposed SDAS Scheme

After validating the proposed scheme, it is used to analyze the test system with different cases. Table VII compares various indices such as various cost components of the objective function, energy losses, peak load on SS, and minimum voltage for different cases by proposed stochastic MISOCP formulation. Among different cases, Case-I (when only DGs are considered in the network) results in maximum total operational cost, maximum energy losses, and maximum peak demand on the SS. The total operating costs in Case-II and Case-III are close to each other. Case-VI results in minimum total operational cost, minimum energy losses, minimum peak demand on the SS, and maximum improvement in voltage profile. In Case-VI, the total operational cost is reduced by 14.64%, 5.76%, 5.72%, 1.75%, and 13.09% as compared to Case-I, Case-II, Case-III, Case-IV, and Case-V, respectively. Further, in Case-VI, the energy losses are reduced by 59.01%, 14.45%, 27.44%, 19.25%, and 49.15%, in comparison to Case-I, Case-II, Case-III, Case-IV, and Case-V, respectively. Case-VI improves the minimum voltage in the network to 0.9423 pu. Also, Case-VI results a peak demand of 4.5453 MVA on the SS, which is also minimum among all the cases considered. Based on these observations, it can be concluded that the proposed SDAS scheme (Case-VI) yields more benefits to the utility in terms of economical operation and improved system performance.

By the proposed SDAS scheme, the schedules of BESSs for Case-VI are shown in Fig. 3. In this figure, $+ve$ and $-ve$ values of active power indicate discharging and charging of BESSs, respectively. BESSs are discharged and charged during peak demand and off-peak demand periods, respectively. Total active participation from SLs in Case-VI is shown in Fig. 4. In this figure, $+ve$ and $-ve$ values of active power indicate decrement and increment, respectively, in the load demand of SLs. The load demand of SLs is reduced and increased during peak demand and off-peak demand periods, respectively.

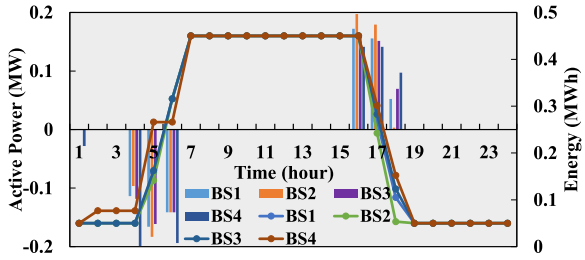

Fig. 3. Schedule of active power and energy of BESSs in Case-VI of stochastic SDAS.

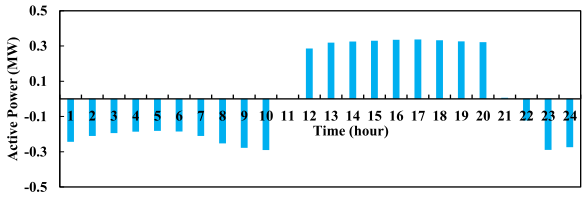

Fig. 4. Total active participation from SLs in Case-VI of stochastic SDAS.

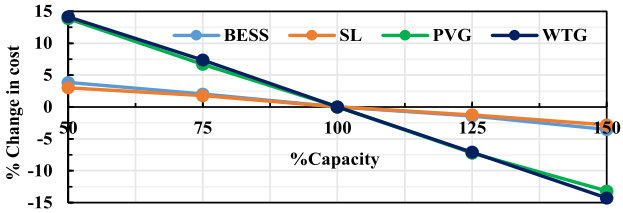

Fig. 5. Sensitivity of total operating cost wrt capacity of active elements.

To check the importance of AEM cost in the proposed formulation, it is excluded from the objective function and the resultant formulation is solved. The observed techno-economic performance of the test network is provided in Table VIII. On comparing the obtained results with Case-VI of Table VII, it is observed that the results of Case-VI are still better. The overall cost, losses, and peak demand on SS become more, if AEM cost is excluded from the objective function. Even though the total AEM cost constitutes a small portion of the overall cost, its inclusion in the objective function results a better solution as seen from Case-VI of Table VII. Thus, it is concluded that AEM costs should be included in the objective function for better techno-economic performance of SDG.

D. Sensitivity Analysis

To analyze the impact of variation in capacity of active elements, namely BESSs, SLs, PVGs, and WTGs, on the overall operating cost, a sensitivity analysis is also conducted. For this purpose, the rating of an active element is varied in a step of 25% from 50% to 150%, and corresponding change in overall operating cost is observed. The 100% capacity, and location of each element are considered same as provided in Table II. Fig. 5 shows percentage change in the total operating cost with respect to (wrt) percentage capacity of active elements. For computing percentage change in the total operational cost, its

TABLE VII
VARIOUS INDICES OF 33-BUS NETWORK WITH STOCHASTIC SDAS

Case	F^{SS} (\$)	F^{BS} (\$)	F^{SCB} (\$)	F^{SL} (\$)	F^{CL} (\$)	F^{CSW} (\$)	F (\$)	Losses (MWh)	Peak demand on SS (MVA)	Minimum voltage (pu)
I	5,664.32	–	–	–	–	–	5,664.32	2.9919	5.6931	0.9028
II	5,098.14	28.71	3.50	–	–	–	5,130.35	1.4337	4.6307	0.9323
III	5,094.72	–	4.50	29.20	0	–	5,128.42	1.6904	4.6404	0.9267
IV	4,859.12	28.69	4.00	29.37	0	–	4,921.18	1.5190	4.5757	0.9336
V	5,522.92	–	–	–	–	40	5,562.92	2.4120	5.5243	0.9055
VI	4,750.70	28.78	4.00	29.18	0	22	4,834.66	1.2265	4.5453	0.9423

TABLE VIII
VARIOUS INDICES OF 33-BUS NETWORK WITH STOCHASTIC SDAS EXCLUDING AEM COST IN OBJECTIVE FUNCTION

Objective	F^{SS} (\$)	F^{BS} (\$)	F^{SCB} (\$)	F^{SL} (\$)	F^{CL} (\$)	F^{CSW} (\$)	F (\$)	Losses (MWh)	Peak demand on SS (MVA)	Minimum voltage (pu)
F^{SS}	4,756.84	28.74	14	32.57	0	32	4,864.15	1.2664	4.7369	0.9389

value, \$4,834.66 obtained from Case-VI of Table VII is taken as the reference. All active elements considered here exhibit a similar trend of sensitivity of the overall cost wrt the change in their capacity. The overall cost decreases with increase in the capacity of active elements and vice-versa. However, PVG and WTG have more impact on the total cost as compared to BESS and SL. This is because about 98% share of the total cost is due to power purchase cost as seen from Case-VI of Table VII. When the capacity of PVG and WTG is increased, it offsets the energy purchased from the grid, and thereby, reduces the total cost. Further, even though the total capacity of PVG is twice that of WTG as seen from Table II, their capacity variation shows almost similar variation in total cost. This is due to nonavailability of PVG during night time. On the other hand, BESS stores the energy during off-peak hours and delivers the same during peak hours as seen from Fig. 3. Thus, it has almost negligible contribution to change in energy purchased from the grid with its capacity variation. However, due to different electricity prices during peak and off-peak hours, it has very small impact on overall cost as reflected in Fig. 5. If the electricity price was made flat, the overall cost would no longer be sensitive to the change in the capacity of BESS. A similar discussion can be also made for SL based on Fig. 4.

VI. CONCLUSION

This study proposes a stochastic SDAS scheme for SDGs to operate their active elements, such as BESSs, SCBs, SLs, CLs, and CSWs, in an optimal manner. For this, a two-stage stochastic and convex MISOCP optimization problem is formulated which seeks to minimize the daily operational cost of SDG. The uncertainties in renewable generation, load, and grid electricity price have been taken into consideration using MCS and a k-means clustering approach. The proposed SDAS scheme is tested on a modified IEEE 33-bus SDG to verify its effectiveness under different cases. It is observed that the available commercial solvers fail to solve the developed formulation within a given time. Therefore, Benders decomposition is employed to obtain an optimal solution with reduced computational time. The results of the proposed SDAS scheme have been compared with those of similar existing works. The comparison indicates a significant techno-economic improvement in the overall performance of SDG with the proposed SDAS. Therefore, the proposed SDAS is proven to be an effective tool for an SDG regarding techno-economic performance under DMS. Further, it is a computationally efficient tool. It can be used by DNOs to determine the dispatch strategies for various active elements and thereby ensuring an efficient operation of SDGs.

REFERENCES

[1] S. Golshannavaz, S. Afsharnia, and F. Aminifar, "Smart distribution grid: Optimal day-ahead scheduling with reconfigurable topology," *IEEE Trans. Smart Grid*, vol. 5, no. 5, pp. 2402–2411, Sep. 2014.
[2] Y. Zhang, J. Wang, and Z. Li, "Uncertainty modeling of distributed energy resources: Techniques and challenges," *Curr. Sustainable/Renewable Energy Rep.*, vol. 6, pp. 42–51, 2019.
[3] X. Qiao et al., "Optimal scheduling of distribution network incorporating topology reconfiguration, battery energy system and load response," *CSEE J. Power Energy Syst*, vol. 8, no. 3, pp. 743–756, 2022.
[4] R. Zafar, J. Ravishankar, J. E. Fletcher, and H. R. Pota, "Multi-timescale model predictive control of battery energy storage system using conic relaxation in smart distribution grids," *IEEE Trans. Power Syst.*, vol. 33, no. 6, pp. 7152–7161, Nov. 2018.
[5] B. S. K. Patnam and N. M. Pindoriya, "Centralized stochastic energy management framework of an aggregator in active distribution network," *IEEE Trans. Ind. Informat.*, vol. 15, no. 3, pp. 1350–1360, Mar. 2019.
[6] Y. Zheng et al., "Optimal operation of battery energy storage system considering distribution system uncertainty," *IEEE Trans. Sustain. Energy*, vol. 9, no. 3, pp. 1051–1060, Jul. 2018.
[7] K. Vemalaiah, D. K. Khatod, and N. P. Padhy, "Optimal day-ahead scheduling for active distribution network considering uncertainty," in *Proc. IEEE Int. Conf. Power Electron. Drives Energy Syst.*, 2022, pp. 1–6.
[8] H. Gao, J. Liu, and L. Wang, "Robust coordinated optimization of active and reactive power in active distribution systems," *IEEE Trans. Smart Grid*, vol. 9, no. 5, pp. 4436–4447, Sep. 2018.
[9] S. Chen, C. Wang, and Z. Zhang, "Multitime scale active and reactive power coordinated optimal dispatch in active distribution network considering multiple correlation of renewable energy sources," *IEEE Trans. Ind. Appl.*, vol. 57, no. 6, pp. 5614–5625, Nov./Dec. 2021.
[10] A. Baharvandi et al., "Linearized hybrid stochastic/robust scheduling of active distribution networks encompassing PVs," *IEEE Trans. Smart Grid*, vol. 11, no. 1, pp. 357–367, Jan. 2020.
[11] V. C. Pandey, N. Gupta, K. R. Niazi, A. Swarnkar, T. Rawat, and C. Konstantinou, "A bi-level decision framework for incentive-based demand response in distribution systems," *IEEE Trans. Energy Markets, Pol. Reg.*, vol. 1, no. 3, pp. 211–225, Sep. 2023.
[12] C. Crozier, A. Pigott, and K. Baker, "Price perturbations for privacy preserving demand response with distribution network awareness," *IEEE Trans. Smart Grid*, vol. 15, no. 2, pp. 1584–1593, Mar. 2024.
[13] K. Wang, C. Wang, Z. Zhang, and X. Wang, "Multi-timescale active distribution network optimal dispatching based on SMPC," *IEEE Trans. Ind. Appl.*, vol. 58, no. 2, pp. 1644–1653, Mar./Apr. 2022.

[14] H. Sheng, C. Wang, B. Li, J. Liang, M. Yang, and Y. Dong, "Multi-timescale active distribution network scheduling considering demand response and user comprehensive satisfaction," *IEEE Trans. Ind. Appl.*, vol. 57, no. 3, pp. 1995–2005, May/Jun. 2021.
[15] S.-M. Razavi, H.-R. Momeni, M.-R. Haghifam, and S. Bolouki, "Multi-objective optimization of distribution networks via daily reconfiguration," *IEEE Trans. Power Del*, vol. 37, no. 2, pp. 775–785, Apr. 2022.
[16] H. M. Ahmed, M. H. Ahmed, and M. Salama, "A linearized multiobjective energy management framework for reconfigurable smart distribution systems considering BESSs," *IEEE Sys. J.*, vol. 16, no. 1, pp. 1258–1269, Mar. 2022.
[17] A. Gabash and P. Li, "Active-reactive optimal power flow in distribution networks with embedded generation and battery storage," *IEEE Trans. Power Syst.*, vol. 27, no. 4, pp. 2026–2035, Nov. 2012.
[18] P. Li, D. Xu, Z. Zhou, W.-J. Lee, and B. Zhao, "Stochastic optimal operation of microgrid based on chaotic binary particle swarm optimization," *IEEE Trans. Smart Grid*, vol. 7, no. 1, pp. 66–73, Jan. 2016.
[19] S. Paul and N. P. Padhy, "A new real time energy efficient management of radial unbalance distribution networks through integration of load shedding and CVR," *IEEE Trans. Power Del*, vol. 37, no. 4, pp. 2571–2586, Aug. 2022.
[20] T. Gangwar, N. P. Padhy, and P. Jena, "Energy management approach to battery energy storage in unbalanced distribution networks," *IEEE Trans. Ind. App.*, vol. 60, no. 1, pp. 1345–1356, Jan./Feb. 2024.
[21] L. H. Macedo, J. F. Franco, M. J. Rider, and R. Romero, "Optimal operation of distribution networks considering energy storage devices," *IEEE Trans. Smart Grid*, vol. 6, no. 6, pp. 2825–2836, Nov. 2015.
[22] L. Tziovani, L. Hadjidemetriou, P. Kolios, A. Astolfi, E. Kyriakides, and S. Timotheou, "Energy management and control of photovoltaic and storage systems in active distribution grids," *IEEE Trans. Power Syst.*, vol. 37, no. 3, pp. 1956–1968, May 2022.
[23] H. Gao, L. Wang, J. Liu, and Z. Wei, "Integrated day-ahead scheduling considering active management in future smart distribution system," *IEEE Trans. Power Syst.*, vol. 33, no. 6, pp. 6049–6061, Nov. 2018.
[24] S. H. Low, "Convex relaxation of optimal power flow–Part I: Formulations and equivalence," *IEEE Trans. Control Netw. Syst.*, vol. 1, no. 1, pp. 15–27, Mar. 2014.
[25] R. A. Jabr, R. Singh, and B. C. Pal, "Minimum loss network reconfiguration using mixed-integer convex programming," *IEEE Trans. Power Syst.*, vol. 27, no. 2, pp. 1106–1115, May 2012.
[26] A. Soroudi and T. Amraee, "Decision making under uncertainty in energy systems: State of the art," *Renewable Sustain. Energy Rev.*, vol. 28, pp. 376–384, 2013.
[27] H. Haghighat and B. Zeng, "Stochastic and chance-constrained conic distribution system expansion planning using bilinear benders decomposition," *IEEE Trans. Power Syst.*, vol. 33, no. 3, pp. 2696–2705, May 2018.
[28] M. E. Cebeci, O. B. Tor, S. V. Oprea, and A. Bára, "Consecutive market and network simulations to optimize investment and operational decisions under different RES penetration scenarios," *IEEE Trans. Sustainable Energy*, vol. 10, no. 4, pp. 2152–2162, Oct. 2019, doi: 10.1109/TSTE.2018.2881036.
[29] R. Manojkumar, C. Kumar, and S. Ganguly, "Optimal demand response in a residential PV storage system using energy pricing limits," *IEEE Trans. Ind. Informat.*, vol. 18, no. 4, pp. 2497–2507, Apr. 2022.
[30] M. Mahdavi, K. E. K. Schmitt, and F. Jurado, "Robust distribution network reconfiguration in the presence of distributed generation under uncertainty in demand and load variations," *IEEE Trans. Power Del.*, vol. 38, no. 5, pp. 3480–3495, Oct. 2023.
[31] K. Vemalaiah, D. K. Khatod, and N. P. Padhy, "An energy efficient network reconfiguration in active distribution network by incorporating losses from converter-based DGs," in *Proc. IEEE Power Energy Soc. Gen. Meeting*, 2023, pp. 1–5.
[32] H. Wu, P. Dong, and M. Liu, "Distribution network reconfiguration for loss reduction and voltage stability with random fuzzy uncertainties of renewable energy generation and load," *IEEE Trans. Ind. Informat.*, vol. 16, no. 9, pp. 5655–5666, Sep. 2020.
[33] C. L. B. Silveira, A. Tabares, L. T. Faria, and J. F. Franco, "Mathematical optimization versus metaheuristic techniques: A performance comparison for reconfiguration of distribution systems," *Electric Power Syst. Res.*, vol. 196, 2021, Art. no. 107272.
[34] D. Arthur and S. Vassilvitskii, "K-means the advantages of careful seeding," in *Proc. 18th Annu. ACM-SIAM Symp. Discrete algorithms*, 2007, pp. 1027–1035.
[35] T. Hong, P. Pinson, Y. Wang, R. Weron, D. Yang, and H. Zareipour, "Energy forecasting: A review and outlook," *IEEE Open Access J. Power Energy*, vol. 7, pp. 376–388, 2020.
[36] A. Shapiro, D. Dentcheva, and A. Ruszczyński, *Lectures on Stochastic Programming*. Society for Industrial and Applied Mathematics, 2009, doi: 10.1137/1.9780898718751.
[37] M. R. Sarker, M. D. Murbach, D. T. Schwartz, and M. A. Ortega-Vazquez, "Optimal operation of a battery energy storage system: Trade-off between grid economics and storage health," *Electric Power Syst. Res.*, vol. 152, pp. 342–349, 2017.
[38] Z. Wei and M. M. Ali, "Generalized benders decomposition for one class of minlps with vector conic constraint," *SIAM J. Optim.*, vol. 25, no. 3, pp. 1809–1825, 2015.
[39] "Renewable-ninja platform." Jan. 2017. [Online]. Available: https://www.renewables.ninja/
[40] A. J. Conejo et al.,, *Decision Making Under Uncertainty in Electricity Markets*, vol. 1. Berlin, Germany: Springer, 2010.

Kasi Vemalaiah (Graduate Student Member, IEEE) received the B.Tech. degree in electrical and electronics engineering from the Audisankara College of Engineering and Technology Gudur, Gudur, India, in 2016, and the M.Tech. degree in power systems engineering from the National Institute of Technology Warangal, Warangal, India, in 2019. He is currently working toward the Ph.D. degree with the Department of Electrical Engineering, Indian Institute of Technology Roorkee, Roorkee, India.

His research interests include optimal planning and operation of the smart distribution grid, renewable energy systems, demand-side management, and uncertainty modeling.

Dheeraj Kumar Khatod (Member, IEEE) received the B.E. degree from the National Institute of Technology (erstwhile Government Engineering College) Raipur, Raipur, India, in 1998, and the M.Tech. and Ph.D. degrees from the Indian Institute of Technology (IIT) Roorkee, Roorkee, India, in 2002 and 2007, respectively, all in electrical engineering.

He is currently an Associate Professor with the Department of Electrical Engineering, IIT Roorkee. His research interests include the planning studies of distributed generation and renewable energy systems, optimal operation of smart distribution grids, and parameter and topology estimation of distribution networks.

Narayana Prasad Padhy (Senior Member, IEEE) received the Ph.D. degree in power systems engineering from Anna University, Chennai, India, in 1997.

He is currently the Director of the Malviya National Institute of Technology, Jaipur, India, and the Mentor Director of the Indian Institute of Information Technology Kota, Kota, India, along with Professor (HAG) (on-lien) with the Department of Electrical Engineering, Indian Institute of Technology (IIT) Roorkee, Roorkee, India. He served as the Dean of Academic Affairs, Institute, NEEPCO, 92 Batch and Ravi Mohan Mangal Institute Chair Professors, IIT Roorkee. He is the National lead of many national and international projects such as DSIDES, ID-EDGe, and HEAPD. He is also part of other international projects, namely Indo-US UI-ASSIST and Indo-U.K. ZED-I. He has authored and coauthored more than 200 research articles in reputed international journals and conference proceedings. His research interests include power system analysis, demand side management, energy market, network pricing, ac–dc smart grid, and application of machine learning techniques in power systems.

Dr. Padhy is also a Fellow of the Indian National Academy of Engineers, Fellow of the Institution of Electronics and Telecommunication Engineers, India, Fellow of the Institution of Engineering and Technology, and Fellow of Institution of Engineers India. He was the recipient of the IEEE Smart Cities Award 2022, IEEE PES Outstanding Engineers Award 2018, Boyscast Fellowship, and the Humboldt Experienced Research Fellowship in the years 2005 and 2009, respectively.